Biosensors and Bioelectronics 71 (2015) 194–199

Contents lists available at ScienceDirect

Biosensors and Bioelectronics

journal homepage: www.elsevier.com/locate/bios

A facile and sensitive electrochemiluminescence biosensor for Hg^{2+} analysis based on a dual-function oligonucleotide probe

Rong-Fu Huang*, Hui-Xin Liu, Qi-Qi Gai, Gai-Juan Liu, Zheng Wei

College of Materials, Chemistry and Chemical Engineering, Chengdu University of Technology, Chengdu, Sichuan 610059, PR China

ARTICLE INFO

Article history:
Received 16 January 2015
Received in revised form
10 April 2015
Accepted 13 April 2015
Available online 14 April 2015

Keywords:
Electrochemiluminescence
Hg^{2+}
$[Ru(bpy)_2(dppz)](BF_4)_2$
DNA biosensor

ABSTRACT

In this study, a sensitive electrochemiluminescent (ECL) biosensor for the detection of Hg^{2+} was easily prepared by self-assembling mercury-specific oligonucleotide on the surface of gold nanoparticles (AuNPs) modified indium tin oxide (ITO) electrode. A conformation change of the oligonucleotide from linear chain to hairpin occurs upon the binding of Hg^{2+} through thymine–Hg^{2+}–thymine coordination. The dual-function oligonucleotide serves as the probe to Hg^{2+} but also a carrier of signal-generating molecules, $[Ru(bpy)_2(dppz)](BF_4)_2$. It was estimated that one oligonucleotide was able to load with eight ECL signal molecules; a ratio of four or five oligonucleotides per gold nanoparticle was obtained basing on the calculation with surface density. Without tedious multiple-labeling procedures and special modification of oligonucleotide probe for signal transduction/amplification, a detection limit of 5.1 pM Hg^{2+} was outstanding from the interference of other ten metal ions. Results of spiked water samples were in good agreement with that obtained by atomic fluorescent spectrometry.

1. Introduction

Hg^{2+} is one of the highly toxic environmental pollutants and is widespread with both natural and anthropologic sources (Driscoll et al. 2013; Wren 1986). Mercury exposures cause many adverse health effects in human and wildlife, even at a low concentration level. Though microbial biomethylation, inorganic mercury can also be converted to methyl mercury which could be accumulated in the body through food chain and show more toxicity than inorganic mercury (Harris et al. 2003). Therefore, the detection of Hg^{2+} with high sensitivity and selectivity is of great importance. Traditionally, the determination of Hg^{2+} can be achieved by atomic fluorescence spectrometry, atomic absorption or emission spectroscopy, inductively coupled plasma-mass spectrometry, and so forth. Although showing high sensitivity, most of these methods cannot widely be applied in routine monitoring due to the complicated sample preparation and expensive instrumentation. In recent years, electrochemiluminescence (ECL) analysis has received considerable attention due to its simple instrument, high detection sensitivity, versatility and robustness (Bard 2004; Hu and Xu 2010). The application of ECL biosensor for the sensitive quantification of ultra-low level of analytes combines the advantages provided by the selectivity of the biological recognition reactions and the high sensitivity of ECL technique (Huang and Guo 2013; Miao 2008).

Currently, Hg^{2+} based DNA-metal base pairs have been widely applied in sensing and molecular nanoarchitectures (Clever et al. 2007). It is found that Hg^{2+} specifically interact with the thymine–thymine (T–T) mismatch in DNA duplexes to form a T–Hg^{2+}–T complex, which was further employed to develop DNA biosensors for the detection of Hg^{2+} (Katz 1952; Liu et al. 2009; Zhang and Guo 2012). The method combination of ECL analysis with the specific T–Hg^{2+}–T construction presents high sensitivity and selectivity for Hg^{2+} analysis. Yin et al. developed an ECL sensor for detecting Hg^{2+} using the DNA/$Ru(phen)_3^{2+}$ (phen=phenanthroline) conjugate as multiple labels which was attached to thymidine-riched oligonucleotide on electrode surface by T–Hg^{2+}–T complex (Tang et al. 2010). This method shows 20000-fold higher selectivity for Hg^{2+} than competing metal ions and detection limit is as low as 20 pM. Later, Xu's group reported a label-free supersandwich ECL assay for the detection of sub-nanomolar Hg^{2+} based on T–Hg^{2+}–T co-ordination (Yuan et al. 2011). Although binding with more ECL signal molecules, no further improvement on detection of limit was achieved because of the interstitial space from ECL signal reporter to electrode surface. Zhang et al. utilized $Ru(bpy)_3^{2+}$ derivatives loaded on G4 PAMAM dendrimer as an ECL emitting species and an extremely low detection limit of 2.4 pM was obtained, which, however, suffer from the complicated procedures for fabrication of ECL sensors (Ma et al. 2012). Therefore, it is desirable to develop simple biosensor for detecting Hg^{2+} with high sensitivity. In this report, we developed a Hg^{2+} biosensor through attaching a mercury-specific oligonucleotide on the

* Corresponding author. Fax: + 86 2884078940.
E-mail address: huangrongfu13@cdut.cn (R.-F. Huang).

http://dx.doi.org/10.1016/j.bios.2015.04.038
0956-5663/

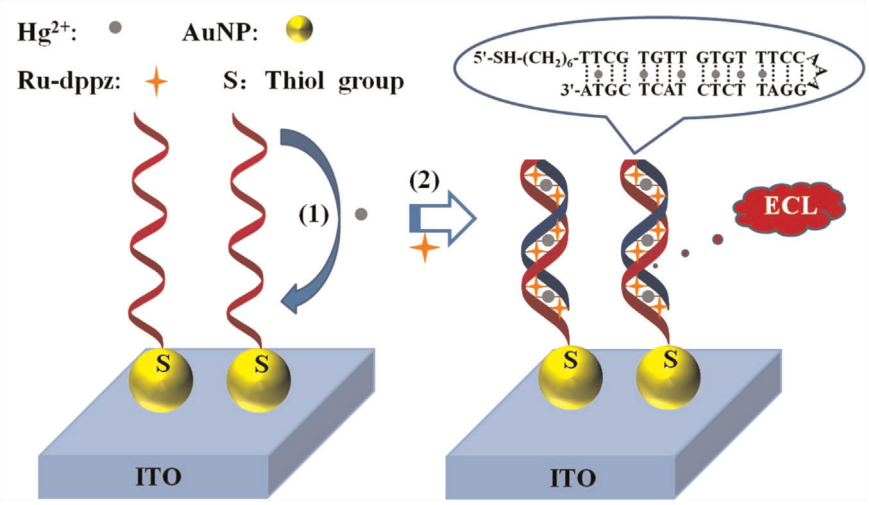

Scheme 1. Schematic diagram of T–Hg^{2+}–T based electrochemiluminescence DNA sensor. (1) Hg^{2+} induced the conformational change of oligonucleotide; (2) Intercalation of ECL indicators into double-stand DNA.

surface of ITO/AuNPs electrode. Scheme 1 illustrated the working principle of the biosensor. The oligonucleotide was designed not only for molecular recognition element, but also to be a carrier for the conjugation of multiple signal reporters.

2. Material and method

2.1. Materials and Reagents

$[Ru(bpy)_2(dppz)](BF_4)_2$ (bpy=2′,2′-bipyridine, dppz=dipyrido [3,2-a:2′,3′-c] phenazine, denoted as Ru-dppz) was synthesized according to the published procedure (Amouyal et al. 1990). *Cis*-Bis-(2,2′-bipyridine)dichlororuthenium(II) dihydrate, o-Phenylenediamine and 1,10-Phenanthroline-5,6-Dione for the synthesis of Ru-dppz and tripropylamine (TPA) were obtained from Aladdin (USA). Hydrogen tetrachloroaurate (*III*) trihydrate ($HAuCl_4 \cdot 3H_2O$), 3-Mercaptopropyltriethoxysilane (MPTES), $Ru(NH_3)_6Cl_3$ and $HS(CH_2)_6OH$ were purchased from J and K Scientific (Beijing, China). The other chemicals were from Kelong Reagent Corporation of Chengdu (China). All the reagents were of analytical-reagent grade without further purification. The synthetic oligonucleotides were acquired from SBS Genetech. Co., Ltd. (China). A concentration of 10 mM phosphate buffer saline (PBS, pH 7.4, 0.10 M NaCl and 10 mM KH_2PO_4/K_2HPO_4) was used to dissolve oligonucleotides.

2.2. Apparatus

The ECL measurement was performed in 150 mM phosphate buffer solution (pH 7.4) containing 100 mM TPA on a Potentiostat PG340 from Eltroscan system (HEKA, Germany) with a Pt counter electrode and an Ag/AgCl (3 M KCl) reference electrode (from CH Instruments, Austin, TX)). ECL intensity was transformed into an electrical signal by an R456 photomultiplier (PMT) (Xi'an Remax Electronic Science Tech. Co. Ltd., Xi'an, China), which was operated at −850 V and the ECL cell was placed directly in front of the PMT. Fluorescence measurements were performed on a F-4600 Fluorescence spectrophotometer (Hitachi, Japan), using 450 nm excitation, and a slit width of 5 nm.

2.3. Fabrication of Hg^{2+} biosensor

Firstly, ITO/AuNPs electrode was prepared as described before (Chen and Zu 2007; Huang and Guo 2010). In brief, cleaned ITO electrodes first reacted with 2% (V/V) 3-Mercaptopropyltriethoxysilane (MPTES) in dry ethanol at room temperature overnight with gently shaking. After carefully washed with ethanol and water, the MPTES modified ITO electrode were dried under a stream of nitrogen. The synthesis of gold nanoparticles with diameter of 20 nm followed Frens method (Frens 1973). The attachment of AuNPs on ITO/MPTES was achieved by casting 20 μL of AuNPs solution on an area of about 0.5 cm × 0.6 cm over 4 h. The resulting electrode was washed carefully with copious amount of water, and dried under a stream of nitrogen before use. The electrode is denoted as ITO/AuNPs and characterized by cyclic voltammograms and SEM image (Figure S1 and S2, Supplementary data).

Next, the thiolated ssDNA was attached to the surface of AuNPs through the sulfur–gold linkage. A 10 μL of the oligonucleotides solution with a desired concentration was added on the surface of the above-prepared ITO/AuNPs electrode and incubated for an appropriate time at 37 °C. After carefully washed with 10 mM PBS to remove the unbound oligonucleotides, the electrode was immersed in 0.10 M PBS (0.10 M KH_2PO_4/K_2HPO_4, 0.10 M NaCl, pH=7.4) containing 1.0 mM 6-Mercapto-1-hexanol for 1 h to block the uncovered surface of AuNPs for eliminating the non-specific adsorption and finally rinsed thoroughly with water. They were then kept in 0.10 M PBS until use.

2.4. Measurement

After the immobilization of oligonucleotides on the electrode, a 10 μL solution of Hg^{2+} was cast and reacted with the DNA at 25 °C for 30 min. After rinse, a 10 μL solution of 10 μM Ru-dppz was added on the electrode and reacted for 30 min. Finally, ECL intensity was measured in a solution of 100 mM TPA.

3. Results and discussion

3.1. Design and characterization of the ECL biosensor

Ru-dppz is well-known as a "light-switch" molecule, showing no photo-/ electro-luminescence in aqueous solution but dramatic increase in the presence of double-stranded DNA (Friedman et al. 1990; Hu et al. 2009). Due to the presence of dppz ligand with extended aromatic structure, the binding constant of Ru-dppz with DNA is estimated as 10^6–10^7 M^{-1}, over 100 times higher than

$Ru(phen)^{2+}$ (Huang et al. 2010). This indicates that the stable DNA/Ru-dppz complex involves in much more practicability. Binding ratio of ligand/base pair (bp) of Ru-dppz is two folds greater than that of $Ru(phen)^{2+}$ (ratio=4) in the saturated solution, suggesting a potential to obtain a better sensitivity. Similar to its fluorescence behavior, Ru-dppz shows the negligible ECL emission in aqueous solution and around 1000 times increase after intercalating into the double helical DNA (Hu et al. 2009; Huang et al. 2010). Thus, the application of promising "light-switch" molecule Ru-dppz in DNA sensing system produces dramatic increase of ECL intensity when reacting with double-stand DNA. This allows the detection of much lower concentration of DNA or indirect analysis of ultra-low level of target which has effect on the conformational change of DNA.

According to the accepted ECL reaction mechanism for $Ru(bpy)_3{}^{2+}$ or its derivatives, high concentration of tripropylamine (TPA) was selected as ECL co-reactant when reacting with low concentration of Ru-dppz due to its exclusive popularity. The ECL behaviors of Ru-dppz/DNA in the solution of TPA were shown in Fig. S3 (Supplementary data). We can see that the highest ECL intensity was detected on glass carbon electrode (GCE), while that on ITO/AuNPs is higher than bulk Au and Pt electrode. Instead of GCE, however, ITO/AuNPs electrode was prepared for the fabrication of ECL biosensor for three reasons. One is the advantage of utility of transparent electrode in ECL analysis, reducing the interference to emitted light from the sample matrix and providing the ease for the arrangement of electrodes in ECL cell (Huang et al. 2011). Secondly, the ITO/AuNPs electrode preserved the good optical transparency of the ITO substrate with highly enhanced ECL activity which is comparable to bulk gold electrode. Thirdly, the orientation of the oligonucleotides and steric space are more flexible than that on a flat electrode. This arrangement would provide sensitive Hg^{2+}-dependent ECL enhancement. The fabrication of ITO/AuNPs electrode was achieved through well-established silane surface chemistry with MPTES and later characterized following previous works (Chen and Zu 2007; Huang and Guo 2010). As seen in Figs. S1 and S2 (Supplementary data), it confirmed the presence of spherical AuNPs with an average diameter of ca. 20 nm on the surface of ITO with uniform disperse and the chemical reversibility of the surface reaction. The surface coverage of AuNPs adsorbed from aqueous solution onto ITO calculated to be around $(20 \pm 1.6)\%$ based on the particle number from SEM image $(6.4 \pm 0.5 \times 10^{10}$ AuNPs/$cm^2)$ and particle size.

Fig. 1 shows the ECL curve of DNA sensor after reacted with different concentration of Hg^{2+}. In the absence of Hg^{2+}, the oligonucleotide maintains a single-strand structure, suggesting no base pairs for the intercalation by Ru-dppz. However, a few Ru-dppz molecules might bind to DNA through electrostatic association (Guo et al. 2006). The undetectable ECL emission is attributed to the quench effect on the phenazine nitrogen of the ligand (dppz) from water. In addition, even in the absence of Ru-dppz, electro-oxidation of TPA produces a weak ECL signal (Black curve), which is similar to that in previous reports (Senthil Kumar and Bard 2012). After adding in Hg^{2+}, a hairpin structure DNA is formed through T–Hg^{2+}–T interactions, which facilitates Ru-dppz intercalation, leading to a Hg^{2+} concentration dependent enhancement of ECL response. As expected, the ECL intensity of Ru-dppz increased progressively with the addition of Hg^{2+}, indicating the formation of DNA duplex. In the presence of Hg^{2+}, ECL emission started at about 0.75 V and reached its maximum at 0.91 V. The reaction mechanism has been widely investigated in Bard's group before and can be concluded as the reaction between Ru-dppz and highly reducing intermediate (TPA·), which generated by oxidation of TPA and latter rapid deprotonation on the surface of gold electrode (Bard 2004). Meanwhile, a shoulder peak appears at ca. 1.3 V, which relates to the direct oxidation of Ru-dppz. On the other hand, we found the similar electrochemical behaviors before and after reacting with Hg^{2+} and Ru-dppz (Fig. 1 Inset). The oxidation current started to rise at 0.6 V and its peak potential was 1.1 V. The rather broad anodic wave was primarily due to the direct oxidation of 0.1 M TPA, and the presence of low concentration of Ru-dppz had little influence on the voltammogram behavior, which is similar to that in previous reports (Zu and Bard 2000).

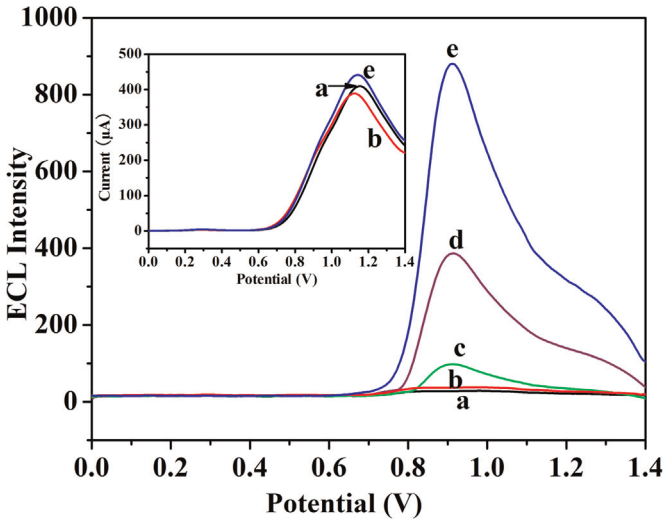

Fig. 1. ECL curve and voltammograms (inset) of 0.1 M TPA in 150 mM PB solution (pH 7.4) at an oligonucleotide modified ITO/AuNPs electrode (curve a), and ITO/AuNPs/ oligonucleotide electrode reacted with varying concentration of Hg^{2+} (0, 0.1, 0.5 and 1 nM, curves b-e), then 10 μM Ru-dppz.

As a promising "light-switch" molecule, Ru-dppz was widely employed as a popular fluorescent probe in DNA detection and structure analysis. Here, fluorescence spectroscopy of Ru-dppz was used to confirm the conformational change of oligonucleotides induced by Hg^{2+}. Due to the relative low sensitivity compared to the ECL technique, higher concentration of Hg^{2+} was added to the solution of oligonucleotide for monitoring the change of fluorescence intensity. In theory, oligonuleotide probe might form a helical structure when reacting with an aqueous solution containing Hg^{2+}, which would provide more binding sites for fluorescence intercalators, resulting in photoluminescent enhancement. Here, low concentration of oligonuleotide is used to avoid the cross-hybridization reaction between two oligonucleotide molecules in the absence of Hg^{2+}, producing low background signal. As expected, no fluorescence emission is detected from Ru-dppz with single stand DNA (Fig. 2). The fluorescence intensity of Ru-dppz on oligonuleotide increased with the addition of Hg^{2+}, also indicating the formation of double-stand DNA.

3.2. *Selection of Hg^{2+}-specific oligonucleotide probe*

ECL emission of Ru-dppz bound to five types of oligonucleotide in the absence/presence of Hg^{2+} were investigated, including a T-rich oligonucleotide (Probe T, 5′-SH-$(CH_2)_6$-$(T)_{24}$-3′), an A-rich oligonucleotide (Probe A, 5′-SH-$(CH_2)_6$-$(A)_{24}$-3′), and mercury-specific oligonucleotides with different chain length (Probe 1-3: 5′-SH-$(CH_2)_6$-TTCG TGTG AAA CACT CGTA-3′; 5′-SH-$(CH_2)_6$-TTCG TGTT GTGT TTCC AAA GGAT TCTC TACT CGTA-3′) and 5′-SH-$(CH_2)_6$-TTCG TGTT GTGT TTCC TGTT TGCG AAA CGCA TTCA GGAT TCTC TACT CGTA-3′). After reacting with Hg^{2+}, the strongest ECL intensity was observed on Probe 3 (Fig. S4, Supplementary data), which is attributed to the formation of longest double-stand

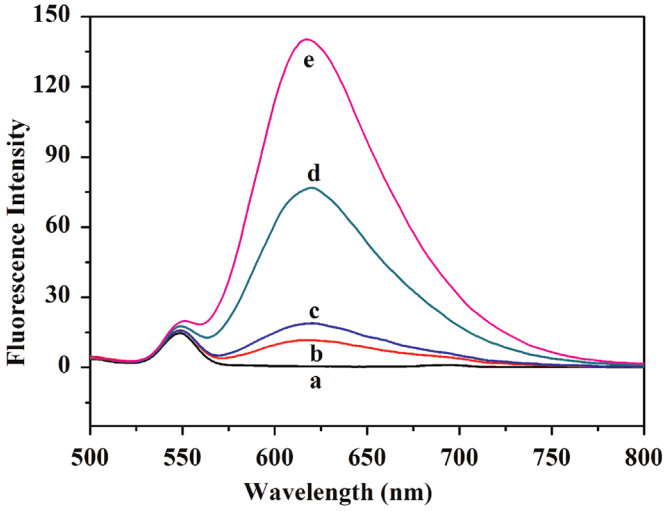

Fig. 2. Fluorescence spectra of a mixture of 0.1 μM oligonucleotide probe 2 and 10 μM Ru-dppz after reacting with 0(a), 0.5(b), 1(c), 2(d), 5(e) nM Hg^{2+}.

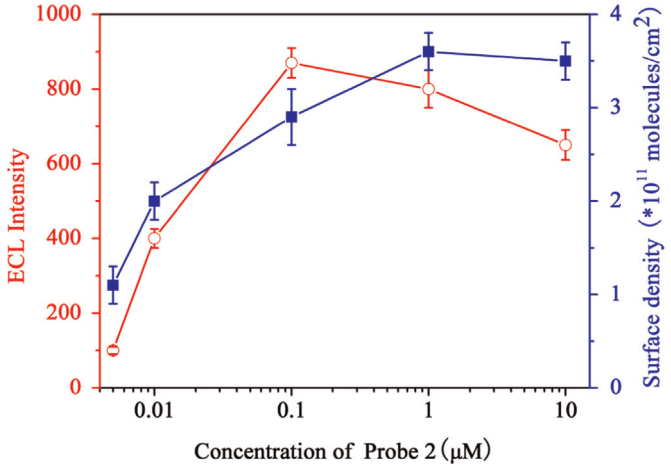

Fig. 3. Effects of concentration on oligonucleotide probe surface density (closed squares) and ECL intensity (open circles).

section for the intercalation of maximal worth of ECL signal reporters. However, the highest blank control signal on Probe 3 can also be explained by longest DNA chain, in which double-stranded structure was partially formed to provide binding site for Ru-dppz in the absence of Hg^{2+}. Conversely, Probe A cannot form the helical structure in the presence of Hg^{2+}, resulting in undetectable ECL emission. Considering the blank signal in the absence of Hg^{2+}, Probe 2 shows a high enough ECL intensity and higher signal-to-noise ratio when compared to Probe 1, 3 and Probe T. Therefore, Probe 2 was selected for sensor development and eight Ru-dppz molecules, theoretically, can be intercalated into each folded oligonucleotide probe after reacting with Hg^{2+}.

3.3. Effects of the concentration of oligonucleotide probe

In ECL biosensor, the immobilization of dual-function oligonucleotide probe on the surface of a transducer plays an important role on the ECL response. Here, the oligonucleotide was successfully attached to the surface of ITO/AuNPs through a self-assembly process and qualitative characterized in 1 mM $K_3[Fe(CN)_6]$ (Fig. S5, Supplementary data). The increase in irreversibility for $K_3[Fe(CN)_6]$ is due to repulsive electrostatic interactions impeding the ability of anions to reach the electrode surface, indicating the presence of oligonucleotide on the surface of ITO/AuNPs electrode. Theoretically, the surface density of oligonucleotide can be adjusted by control of the self-assembly time and reaction concentration. Here, the concentrations of the oligonucleotide were optimized at long enough self-assembly time (4 h or more) after reached the adsorption equilibrium at each concentration. From Fig. 3 (Blue curve), it can be seen that the oligonucleotide density increased with the concentration of oligonucleotide up to 1 μmol/L, and then levels off at higher oligonucleotide concentration. The plateau indicates saturation of oligonucleotide immobilization. The amount of DNA immobilized on the surface of ITO/AuNPs electrode from $1.1 \pm 0.2 \times 10^{11}$ to $3.6 \pm 0.3 \times 10^{11}$ molecules/cm^2 was characterized by chronocoulometry in 10 mM Tris–HCl containing 50 mM $[Ru(NH_3)_6]^{3+}$ according to the method employed previously (Steel et al. 1998). However, after reacted with Hg^{2+} and Ru-dppz, ECL intensity increases with increasing self-assembly concentration from 0.005 to 0.1 μM, which was attributed to the increase of probe density. With further increase in the self-assembling concentration, ECL intensity conversely decreased (Fig. 3, Red curve). This phenomenon can be reasonably explained by steric and electrostatic hindrance arising from the more tightly packed probe and some interstitial space between the probes, which are necessary for conformational change to hairpin structure and intercalation of Ru-dppz (Zhang et al. 2008). Therefore, the self-assembly concentration of 100 nM was employed for oligonucleotide immobilization, and the amount of DNA is calculated to be $2.9 \pm 0.3 \times 10^{11}$ molecules/cm^2 (Fig. S6, Supplementary data). Based on the number of gold nanoparticles on ITO substrate ($6.4 \pm 0.5 \times 10^{10}$ AuNPs/cm^2), it can be calculated that around 4–5 oligonucleotides molecules were attached to each AuNP on average. Due to the possibility of cross interaction between two oligonucleotide molecules, some binding sites can be provided for Ru-dppz intercalation in the absence of Hg^{2+}, producing high background emission. Combination with interstitial space of AuNPs and particle size, the negligible blank signal in Fig. 1 can be partially explained by the low surface density of probes.

3.4. Analytical performance and interference study

The calibration plot of the sensor under the optimized experimental conditions is shown in Fig. 4. The calibration range of Hg^{2+} was done from 0.02 to 30 nM. ECL intensity initially increases with Hg^{2+} concentrations up to 20 nM, and then levels off at higher

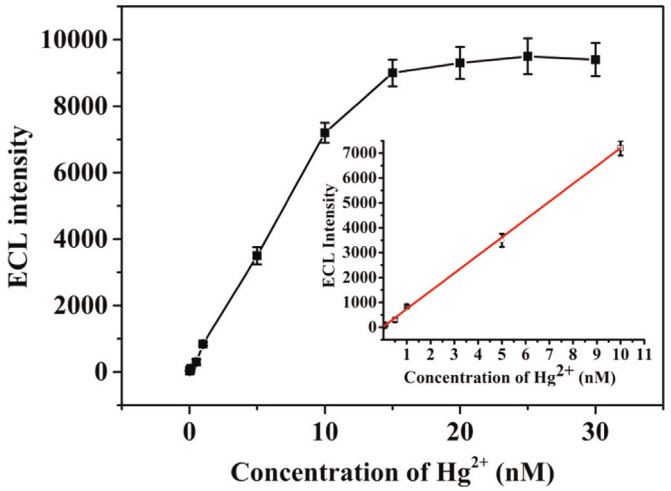

Fig. 4. Relationship between the ECL intensity and concentration of Hg^{2+}. Inset: linear calibration plot for Hg^{2+} detection.

Table 1
Detection of Hg^{2+} in water samples using the proposed method and AFS.

Sample	Added (nM)	Proposed method (nM)[a]	Recovery (%)	AFS (nM)[a]
Tap water	0	n.d.[b]	n.d.	n.d.
	0.10	0.11 ± 0.03	110	n.d.
	0.50	0.51 ± 0.04	102	n.d.
Lake water	0	0.61 ± 0.04	n.d.	n.d.
	4.00	4.89 ± 0.05	107	4.79 ± 0.13
	8.00	8.39 ± 0.27	97	8.86 ± 0.31

[a] Mean of three measurements with standard deviation.
[b] N.d.: not detectable.

Hg^{2+} concentrations. The plateau indicates saturation of Hg^{2+} binding sites on the oligonucleotide probe 2. The linear response range of the sensor to Hg^{2+} concentration was from 5.0×10^{-11} to 1.0×10^{-8} M, and the regression equation was $I_{ECL}=717.9C+25.44$ ($R^2=0.9968$), where the concentration (C) is measured in 10^{-9} M (Fig. 4, inset). The relative standard deviation for seven replicate measurements of 1×10^{-9} nM of Hg^{2+} is 8.7%. A satisfactory reproducibility of the proposed method is observed. To assess the selectivity of the proposed method, interference from various metal ions (Ca^{2+}, Cd^{2+}, Co^{2+}, Cu^{2+}, Fe^{2+}, Mg^{2+}, Mn^{2+}, Pb^{2+}, Al^{3+}, Fe^{3+}) with a 1000-fold concentration higher than Hg^{2+} were examined. As shown in Fig. S7 (Supplementary data), the presence of interference shows the substantially lower ECL intensity than with Hg^{2+}. The slightly change of ECL emission in the presence of a mixture solution containing 1.0×10^{-9} M Hg^{2+} and other metal ions is negligible. The excellent selectivity for the detection of Hg^{2+} is clearly attributed to its selective binding to thymines, resulting in the formation of stable T–Hg^{2+}–T complexes.

3.5. Regeneration and practical applications

The regeneration ability of the ECL sensors is critically important for the sensor applications, which was tested following previous method (Han et al. 2009). In brief, the biosensor was regenerated after incubating the used electrode in the solution of 10 μM cysteine for 1 h to remove Hg^{2+} from the T–Hg^{2+}–T base pairs, as cystein-Hg^{2+} complex shows much higher affinity constant than the T–Hg^{2+}–T complex. A value of ca. 30–40% of the decrease was observed. The decrease can be attributed to the formation of surface oxides and the loss of the probe molecules from the electrode surface (Bard 2004; Du et al. 2005). To solve this problem, small amounts of halide species or low concentration of surfactant can be used to inhibit the growth of surface oxides (Bard 2004). In addition, investigation of stronger covalent bonding to the electrode to enhance the regeneration ability is in progress.

The applicability of the sensor to detect Hg^{2+} in aqueous samples were explored by measuring Hg^{2+} spiked into tap water and lake water, which have been determined by atomic fluorescent spectrometry (AFS) as well. Lake water sample was obtained from Yanhu Lake in campus, Chengdu University of Technology. The samples collected were filtered through 0.2 μm membranes to remove impurities. As shown in Table 1, the recoveries ranged from 97 to 110% for samples spiked with different amount of Hg^{2+} ions. The results were in good agreement with those obtained by AFS, showing the potential practicality of the sensor for real samples.

4. Conclusions

In summary, a label-free ECL biosensor for detecting picomolar Hg^{2+} was one-step constructed and successfully applied to measure Hg^{2+} in aqueous samples. The application of "light-switch" molecule, Ru-dppz, in DNA sensor as ECL signal reporter shows ca. 4-fold lower detection limit than the method using $Ru(phen)_3^{2+}$ as ECL probe. This can be reasonably explained by the higher binding stoichiometry with DNA and "light-on" feature in the presence of double helical DNA, producing dramatic increase in ECL intensity upon intercalation. This result is also comparable to Zhang's work (Ma et al. 2012) but without complicated experimental procedures for the preparation of ECL probe. In theory, the introduction of surfactant or halide ions into ECL measurement can increase the detection sensitivity. Furthermore, the sensor can easily be extended to detecting other metal ions when in combination with the reported metal-base pairs.

Acknowledgments

This work was supported by the National Natural Science Foundation of China (Grant no. 21407013), and General Project for the Cultivation of Talents in Higher Education and Teaching Reform (No. 13JGY07).

Appendix A. Supplementary material

Supplementary data associated with this article can be found in the online version at http://dx.doi.org/10.1016/j.bios.2015.04.038

References

Amouyal, E., Homsi, A., Chambron, J.-C., Sauvage, J.-P., 1990. Synthesis and study of a mixed-ligand ruthenium(II) complex in its ground and excited states: bis(2,2′-bipyridine)(dipyrido[3,2-a: 2′,3′-c]phenazine-N^{4}N^5)ruthenium(II). J. Chem. Soc. Dalton Trans. (6), 1841–1845.
Bard, A.J., 2004. Electrogenerated Chemiluminescence. Marcel Dekker, New York.
Chen, Z.F., Zu, Y.B., 2007. Gold nanoparticle-modified ITO electrode for electrogenerated chemilumineseence: well-preserved transparency and highly enhanced activity. Langmuir 23 (23), 11387–11390.
Clever, G.H., Kaul, C., Carell, T., 2007. DNA-metal base pairs. Angew. Chem. Int. Ed. 46 (33), 6226–6236.
Driscoll, C.T., Mason, R.P., Chan, H.M., Jacob, D.J., Pirrone, N., 2013. Mercury as a global pollutant: sources pathways, and effects. Environ. Sci. Technol. 47 (10), 4967–4983.
Du, H., Strohsahl, C.M., Camera, J., Miller, B.L., Krauss, T.D., 2005. Sensitivity and specificity of metal surface-immobilized "molecular beacon" biosensors. J. Am. Chem. Soc. 127 (21), 7932–7940.
Frens, G., 1973. Controlled nucleation for regulation of particle-size in monodisperse gold suspensions. Nat.-Phys. Sci. 241 (105), 20–22.
Friedman, A.E., Chambron, J.C., Sauvage, J.P., Turro, N.J., Barton, J.K., 1990. Molecular "light switch" for DNA: $Ru(bpy)_2(dppz)^{2+}$. J. Am. Chem. Soc. 112 (12), 4960–4962.
Guo, L.H., Wei, M.Y., Chen, H., 2006. Multiple DNA binding modes of a metallointercalator revealed by DNA film voltammetry. J. Phys. Chem. B 110 (41), 20568–20571.
Han, B., Yuan, J., Wang, E., 2009. Sensitive and selective sensor for biothiols in the cell based on the recovered fluorescence of the CdTe quantum dots-Hg(II) system. Anal. Chem. 81 (13), 5569–5573.
Harris, H.H., Pickering, I.J., George, G.N., 2003. The chemical form of mercury in fish. Science 301 (5637) 1203-1203.
Hu, L., Xu, G., 2010. Applications and trends in electrochemiluminescence. Chem. Soc. Rev. 39 (8), 3275–3304.
Hu, L.Z., Bian, Z., Li, H.J., Han, S., Yuan, Y.L., Gao, L.X., Xu, G.B., 2009. $[Ru(bpy)_2dppz]^{2+}$ electrochemiluminescence switch and its applications for DNA interaction study and label-free ATP aptasensor. Anal. Chem. 81 (23), 9807–9811.
Huang, R., Guo, L.-H., 2010. Lack of nano size effect on electrochemistry of dopamine at a gold nanoparticle modified indium tin oxide electrode. Sci. China Chem. 53 (8), 1778–1783.
Huang, R., Guo, L.-H., 2013. Nanomaterial-Based Electrochemiluminescence Biosensors In: Li, J., Wu, N. (Eds.), Biosensors Based on Nanomaterials and

Nanodevices. CRC Press, Florida, pp. 209–240.
Huang, R., Wang, L.-R., Guo, L.-H., 2010. Highly sensitive electrochemiluminescence displacement method for the study of DNA/small molecule binding interactions. Anal. Chim. Acta 676 (1), 41–45.
Huang, R.F., Wei, M.Y., Guo, L.H., 2011. Enhanced electrogenerated chemiluminescence of $Ru(bpy)_3^{2+}$/tripropylamine system on indium tin oxide nanoparticle modified transparent electrode. J. Electroanal. Chem. 656 (1–2), 136–139.
Katz, S., 1952. The reversible reaction of sodium thymonucleate and mercuric chloride. J. Am. Chem. Soc. 74 (9), 2238–2245.
Liu, S.-J., Nie, H.-G., Jiang, J.-H., Shen, G.-L., Yu, R.-Q., 2009. Electrochemical sensor for mercury (II) based on conformational switch mediated by interstrand cooperative coordination. Anal. Chem. 81 (14), 5724–5730.
Ma, F., Zhang, Y., Qi, H., Gao, Q., Zhang, C., Miao, W., 2012. Ultrasensitive electrogenerated chemiluminescence biosensor for the determination of mercury ion incorporating G4 PAMAM dendrimer and Hg (II)-specific oligonucleotide. Biosens. Bioelectron. 32 (1), 37–42.
Miao, W., 2008. Electrogenerated chemiluminescence and its biorelated applications. Chem. Rev. 108 (7), 2506–2553.
Senthil Kumar, S., Bard, A.J., 2012. Background emission of electrogenerated chemiluminescence during oxidation of Tri-n-propylamine from the dimeric $^1\Delta_g$ State of O_2. Anal. Chem 85 (1), 292–295.
Steel, A.B., Herne, T.M., Tarlov, M.J., 1998. Electrochemical quantitation of DNA immobilized on gold. Anal. Chem. 70 (22), 4670–4677.
Tang, C.-X., Zhao, Y., He, X.-W., Yin, X.-B., 2010. A "turn-on" electrochemiluminescent biosensor for detecting Hg^{2+} at femtomole level based on the intercalation of $Ru(phen)_3^{2+}$ into ds-DNA. Chem. Commun. 46 (47), 9022–9024.
Wren, C.D., 1986. A review of metal accumulation and toxicity in wild mammals: I. Mercury. Environ. Res. 40 (1), 210–244.
Yuan, T., Liu, Z., Hu, L., Zhang, L., Xu, G., 2011. Label-free supersandwich electrochemiluminescence assay for detection of sub-nanomolar Hg^{2+}. Chem. Commun. 47 (43), 11951–11953.
Zhang, B., Guo, L.-H., 2012. Highly sensitive and selective photoelectrochemical DNA sensor for the detection of Hg^{2+} in aqueous solutions. Biosens. Bioelectron. 37 (1), 112–115.
Zhang, J., Qi, H., Li, Y., Yang, J., Gao, Q., Zhang, C., 2008. Electrogenerated chemiluminescence DNA biosensor based on hairpin DNA probe labeled with ruthenium complex. Anal. Chem. 80 (8), 2888–2894.
Zu, Y.B., Bard, A.J., 2000. Electrogenerated chemiluminescence. 66. The role of direct coreactant oxidation in the ruthenium tris(2,2′)bipyridyl/tripropylamine system and the effect of halide ions on the emission intensity. Anal. Chem. 72 (14), 3223–3232.